ZIBELINE INTERNATIONAL™ PUBLISHING

ISSN: 2682-7786 (Online)
CODEN: BDAIDR

Big Data in Agriculture (BDA)

DOI: http://doi.org/10.26480/bda.01.2023.01.05

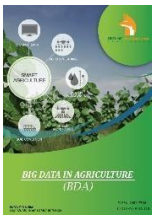

RESEARCH ARTICLE

AN IMAGE PROCESSING APPROACH FOR MONITORING SOIL PLOWING BASED ON DRONE RGB IMAGES

Hasbi Mubarak Suud

Study Program of Agricultural Science, University of Jember, Bondowoso District, Indonesia
Corresponding Author Email: hasbimubarak@unej.ac.id

ARTICLE DETAILS

Article History:

Received 21 October 2022
Revised 01 November 2022
Accepted 02 December 2022
Available online 06 December 2022

ABSTRACT

Soil tillage is a crucial stage in growing plants. Plant roots need soil cavities with good aeration which is obtained from an excellent soil-plowing process. Controlling the quality of plowing process should be done quickly and precisely since it affects the planting schedule and seed handling in the field. Monitoring the plowing area using drone is the best way since it has low-cost operations and is easy to operate. Most drones used today are equipped with a CMOS camera sensor that produces RGB images with good resolution. This study tries to maximize these RGB images to analyze the plowing area and plowing depth using the vegetative indices formulas and GLCM function. Vari formula is the best vegetive indices compared with VIgreen and GLI formula that can be used to distinguish plowed and unplowed areas in this study. The segmentation algorithm which was developed in this study can detect the plowing area. Based on the test, the segmentation algorithm can detect the plowed area, and the results have been compared with manual observation. The correlation coefficient (r) between the result of the segmentation algorithm and manual observation is 0.77. The composition of RGB in each pixel influences the algorithm's performance to distinguish the plowed and unplowed areas. However, the GLCM function is not strong enough to estimate the plowing depth because the correlation coefficient is very weak.

KEYWORDS

Image Processing; Segmentation Algorithm; GLCM; Vegetative Index; Plowed Area

1. INTRODUCTION

The quality of soil tillage ensures the plant roots can develop and breathe, so that is important to make sure this process is well executed. Soil tillage characteristics, including a method, deep tillage, repetition period, and type of tillage machine, can influence the yields (Shamsabadi, 2008; ALkhafaji et al., 2018). However, monitoring and evaluating soil tillage are challenging, especially in large-scale and remote operating areas. In developed countries like Indonesia, many plantation and agriculture locations are located in remote places on the island of Kalimantan, Sumatra, Papua, or Sulawesi, with access that is not easy and tough to pass (Rachmat et al., 1995). These conditions make monitoring land clearing and soil tillage more complex and challenging. There is often a lack of time for monitoring and assessing the soil tillage to catch up with the tight schedule of seedling time, lining, planting, and field maintenance. Ensure the soil tillage work affects not only the planting schedule but also the cost and economic viability (Corley and Tinker, 2015; de Amorim et al., 2021).

Using UAVs for monitoring and evaluating quickly and accurately is a feasible solution. An aerial survey using a drone is fast in collecting aerial imagery data and has a low-cost operation to be conducted at any time. The aerial imagery can be handled to resolve tasks by further image processing (Hartanto et al., 2019). There are two UAV sensors for monitoring land and vegetation, RGB (Red; Green; Blue) and multispectral. The multispectral sensor is more accurate since it has two more spectral bands than the RGB sensor, which only has three. The RGB sensor only has spectral bands: red, green, and blue, whereas the multispectral has two more spectral bands: red-edge and near-infrared. Although the multispectral sensor is more accurate, the RGB sensor is more affordable and accessible (Furukawa et al., 2021).

Most previous studies about processing drone images for agriculture and forestry are based on vegetation indices. Vegetation indices analysis exploits the object reflectance to distinguish vegetation based on light spectra: the ultraviolet region, the visible spectra, and the near-mid infrared band. The difference in object emissivity rate becomes the basis of analysis for quantifying vegetation characteristics like water, sugar, or protein content in leaves (Xue and Su, 2017) . Not only vegetation but soil also has a variance in emissivity rate caused by water content, temperature, compaction, etc. Nir and mid-range infrared are usually used to detect soil characteristics based on thermal radiation (Mira et al., 2007). Hence, using vegetation indices based on RGB images usually has limited utilization compared to multispectral images. Despite that, there is an opportunity to use RGB images for soil analysis since there is a strong correlation between the brightness of RGB and soil moisture content. The more significant brightness of the soil image tends to indicate drier soil (Al-Naji et al., 2021).

This study focused on establishing an algorithm model to compute the area and approximate the depth of cultivated land based on drone RGB images since the RGB drone image is more accessible and can be reached by farmers, especially local farmers in remote areas. The hope is that the farmers can easily quantify the plowing results based on RGB drone image data objectively and rapidly. The principle of plowing is how to break up and flip the soil to create more loose soils and air cavities. The soil in the lower layer with more moisture will be lifted during the plowing and make a different appearance on the ground. This different appearance is used to distinguish the plowed and unplowed soil. The previous study concerning image processing images to evaluate soil tillage focused on detecting soil surface roughness after plowing using two CCD sensor cameras (Riegler et al., 2014). The technique was developed further to analyze the surface roughness using stereo vision, the two cameras are put on top of the soil

Quick Response Code	Access this article online	
	Website: www.bigdatainagriculture.com.my	**DOI:** 10.26480/bda.01.2023.01.05

plowing, and the images captured are processed using stereo matching (Riegler et al., 2020). However, those methods are not easy to apply, although the techniques have high accuracy. There is another technique to process image data from a drone that is more simple to apply. To used the light drone with a CMOS sensor to evaluate the soil tillage by analyzing the texture of the images (Fanigliulo et al., 2020). This method seems capable of presenting a general relationship with the old technique by introducing Gray Level Co-Occurrence (GLCM) and Angular Second Moment (ASM) formulas to analyze the images.

This study uses two methods as base development: vegetative indices and gray level co-occurrence (GLCM) function. The vegetative indices are used for detecting plowed land areas and the GLCM is used for calculating plowing depth to estimate the plowing depth. There are three vegetative indices explored in this study: visible atmospherically resistant index (Vari) visible atmospherically resistant indices green (VIgreen) and green leaf index (GLI). The Vari, VIgreen, and GLI formulas were initially used to capture vegetation data in varying conditions and equipment. Those three formulas only use the index value of spectral bands red, green, and blue for processing (Eng et al., 2019). Vari formula works for estimating the fraction of vegetation with minimal sensitivity to atmospheric effects. Thus the VIgreen is used to interpret ground cover and identify soil, green foliage, snow, or water (Gitelson et al., 2002). GLI formula is sensitive to greenish leaves and can distinguish soil and leaf by the resulting number. If the value is negative, it indicates soil; otherwise, if the value is positive, it indicates green leaves (Louhaichi et al., 2008). Those three vegetative indices have one thing in common: detecting vegetation and can distinguish between vegetation and the soil.

The GLCM function characterizes an image's texture by calculating how often pairs of pixel with specific values and in a specified spatial relationship occur in an image. The GLCM has been used widely to extract second-order statistical texture features for the motion estimation of images. There are essential statistical features to calculate the image texture: entropy, energy, and homogeneity (Mohanaiah et al., 2013). The image texture characteristic has a chance to correlate with plowing depth since the plowed soil generates mound of soil left over from tillage. It has determined the chance to use K-Nearest Neighbor (KNN) and GLCM to classify which land area has been plowed and which has not, but the accuracy of this method is still low (Setiyono et al., 2022; Meng et al., 2020) indicated a high accuracy rate of using GLCM and soil electrical conductivity measurement to predict soil texture. However, previous study revealed that there are redundancy results from GLCM functions to distinguish soil type by (Beliakov et al., 2008). Moreover, this study discusses the feasibility and possibilities of developing algorithm to detect the plowed area based on the vegetative indices formula and to estimate the plowing depth based on GLCM function for monitoring and evaluating soil tillage work.

2. Material and Method

2.1 Study Area

The soil tillage activity was conducted in the experiment field at the University of Jember college in Bondowoso District, Indonesia (7°54'06.8 "S 113°48'16.1 "E). The DJI Phantom 4 Pro was used for acquiring aerial image data that has 1 inch CMOS RGB sensor, which reaches the red, green, and blue wavelength. A tractor with 36 HP installed with disc plow implements and a two-wheel tractor with 8,5 HP installed with mould plow implements were used in this study to give soil tillage treatment on the field.

2.2 Data Gathering

The drone flew between 40 to 50 meters to take images with the camera position perpendicular to the ground surface. The images were saved in JPEG format and used as initial images for testing the segmentation process to recognize the cultivated land. The initial images used for testing represented a wide range of land conditions to ensure the segmentation process can work in various vegetation conditions. The initial pictures used in this study are shown in Figure 1. The description for each initial image is written in Table 1.

Data field officers take the plowed area data and depth of plowing data on the ground to evaluate the performance of the image processing algorithm. They also verified and marked border points of the plowed area and inputted those points into ImageJ software to calculate the size of the plowed area. The plowed area data is the percentage of pixels that indicate the area cultivated to whole number pixels of the image as shown in Eq 1. The plowed area and depth of plowing data that data field officers took are used to assess the correlation between data gathered in the field and the result of the image processing algorithm.

$$plowed\ area\ (\%) = \frac{number\ of\ pixels\ of\ plowed\ area}{total\ number\ of\ image\ pixels} x100\% \quad \text{(Eq 1)}$$

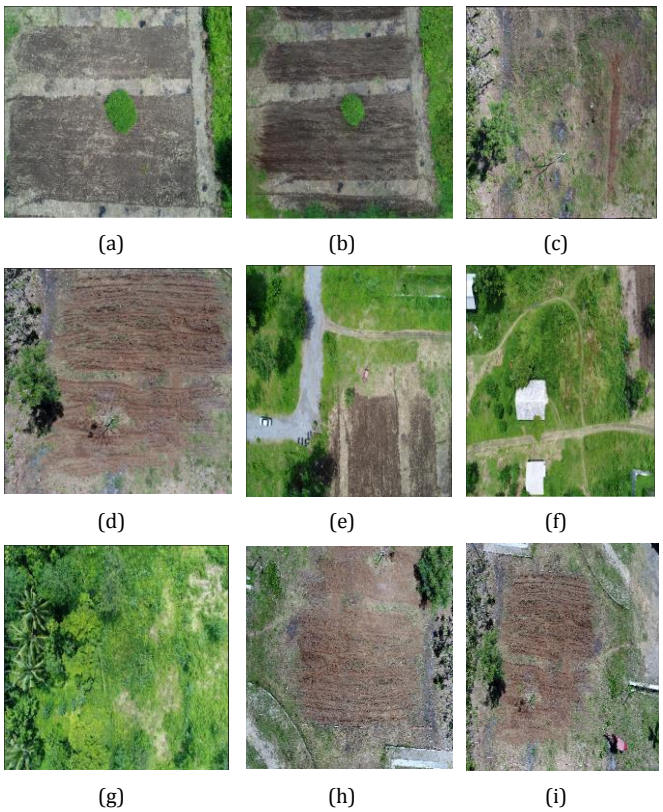

Figure 1: The initial image was taken using drone for segmentation process

Table 1: description of land conditions in Figure 1	
Figure	Description
1(a)	The land after plowed with a moldboard plow.
1(b)	The land after plowed with a moldboard plow and followed by disc plows.
1(c)	The land with minimum vegetation
1(d)	The land in Fig 1(c) after plowed with disc plows.
1(e)	The land with grass, road, and plowed soil area
1(f)	The land with vegetation, building, road, and plowed area.
1(g)	Area with vegetation and no-tillage.
1(h)	The land after plowed with disc plows.
1(i)	The land after plowed with disc plows.

2.3 Data Image Processing

The drone images are processed using the Vari, VIgreen, and GLI formulas. The images with three spectral bands Red, Green, and Blue, are converted into a single vegetative index (VI) value, as shown in Eq 2, Eq 3, and Eq 4.

$$Vari = \frac{Green-Red}{Green+Red-Blue} \quad \text{(Eq 2)}$$

$$VIgreen = \frac{Green-Red}{Green+Red} \quad \text{(Eq 3)}$$

$$GLI = \frac{2.Green-Red-Blue}{2.Green+Red+Blue} \quad \text{(Eq 4)}$$

The Vari, VIgreen, and GLI formula generated images with single vegetative index (VI) values between -1 and 1. These images are needed to be classified and converted to each selected representative color to make it easier to recognize using pseudocolor operation. All those image processing algorithms are written in Matlab Software.

2.4 Accuracy Assessment

Correlation coefficient (r) is used to check the accuracy of the method performance. There are two correlation coefficient calculation carried out in this study. The first is to check the result of segmentation algorithm to

calculate the percentage of plowed area. The second correlation coefficient calculation is to see the relation between GLCM parameters with the plowing depth.

3. RESULTS

3.1 Comparison of Three Vegetative Indices

All three kinds of vegetative indices formulas generate a similar result. Almost negative VI values indicate soil objects, although the negative VI can also be scattered in the other objects. But among the three kinds of vegetative indices formulas also have different value ranges for the same object group. For example, using the Vari formula, the suspected cultivated area mostly has VI values between -1 and -0.18, but the GLI formula generates VI between -1 and -0.8. The Vari formula generates a more considerable variation range of negative VI, so the regions indicated as the cultivated area are more apparent than the result of the VIgreen and GLI formulas. Based on this observation, the negative VI value generated from Vari formula is used as base formula for detecting the plowed area in this study.

3.2 Segmentation Algorithm Development

The result of image processing using the Vari, VIgreen, and GLI deliver the vegetative index (VI) value in each pixel. Since we focused on negative VI as based data to measure the plowed area, the pixels with positive VI are removed to clarify the appearance of the suspected cultivated area. It makes only pixels suspected as plowed areas displayed in the image, likes as shown in Figure 2. The negative VI in the image processed with the Vari formula can be reckoned as a plowed area, but some pixels are scattered in the area that shouldn't be plowed area. The area surrounded by the red line, as shown in Figure 2a, is supposed to be detected as unplowed areas though the color in those pixels has negative VI. Furthermore, non-soil objects like a tractor, circled in the blue circle, also have negative VI. Those negative VI can be called unwanted negative VI. So it needs further segmentation process to minimize the unwanted negative VI for identifying the plowed area. The algorithm of the segmentation process should be made from the common characteristic of the plowing process. The plowing process leaves traces in the overlapping area, so the pixels with the negative VI indicating cultivated land should be close to each other. If the pixels with negative VI are spread out, it is most likely not identified as the plowed area.

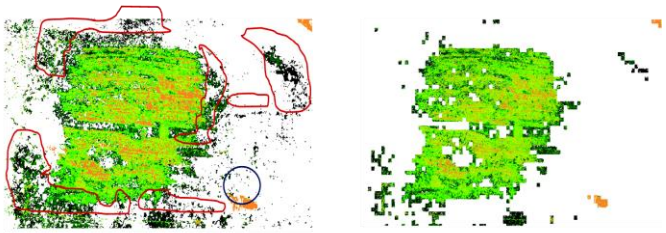

(a) (b)

Figure 2: Distribution of pixels with the negative vegetative index from the initial image in Fig 1.i : (a) the result of the Vari formula; (b) the result of the first segmentation

The first segmentation algorithm is intended to remove the pixels with negative vegetation index (VI) that are not close to each other or can be called unwanted negative VI. The process starts by dividing the image into smaller fragments. If the number of pixels with negative VI is more than half of the total pixels in the image fragment, then the pixels with negative VI are preserved. The image is fragmented into small rectangular areas of nine pixels in size in this illustration. Then the ratio between pixels with negative VI and the total amount of pixels in each fragmented area are calculated using Eq 5. If the ratio of negative VI in the fragmented VI is below 50%, then the pixels with negative VI in the fragmented area are converted to unwanted negative VI. Pixels that are categorized as unwanted negative VI are changed to white pseudocolor. But if the ratio is bigger than 50%, the pixels with negative VI in the fragmented area are kept as suspected plowed areas. The sample images in Figure 2 provide a clearer view of this process. The image in Figure 2(a) is the early distribution of the pixels with negative VI resulting from the Vari Formula. The result of the first segmentation algorithm to eliminate the unwanted negative VI is shown in Figure 2(b), which generates a more precise and accurate plowed area.

$$Ratio\ of\ negative\ VI = \frac{Total\ number\ of\ pixels\ with\ negative\ VI}{Total\ number\ of\ pixels} \quad \text{(Eq 5)}$$

But in some cases, the first segmentation processing doesn't enough to eliminate the unwanted negative VI. The sample image in Figure 3(a) gives an overview of the suspected plowed area that has been processed using the Vari formula from the initial image in Figure 1(c). The actual plowed area is the pixels with brown color inside the black marker line, but there are many unwanted negative vegetative indexes spread almost all over the image. The actual land condition of this image is arid with minimum vegetation, as shown in Figure 1(c). The dry soil tends to have a darker color in the image and generates negative VI. After processing with the first segmentation algorithm, the result showed that there are still so many unwanted pixels with negative VI, as shown in Figure 3(b). Therefore, it needs more in-depth analysis to classify the plowed area. Somehow the development of the first segmentation should be tested for consistency since it will influence the next step decision. The consistency examination compares the result of the first segmentation with different sizes of the image fragments using Eq 6. Suppose the consistency calculation using Eq 6 has a result greater than 1. In that case, the difference between the two results after being processed using the first segmentation is too big and needs further segmentation. Otherwise, further segmentation is not required if the consistency is smaller than 1.

$$Consistency = \frac{(Ratio\ of\ negative\ VI\ (larger\ fragment) - Ratio\ of\ negative\ VI\ (smaller\ fragment))}{Ratio\ of\ negative\ VI\ (larger\ fragment)} \quad \text{(Eq 6)}$$

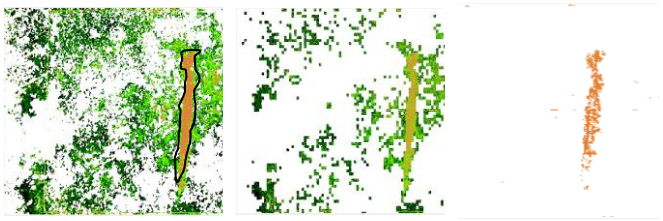

(a) (b) (c)

Figure 3: Distribution of pixels with the negative vegetative index from the initial image in Figure 1(c); (a) outcome of the Vari formula; (b) outcome of first segmentation; (c) outcome of second segmentation

The second segmentation algorithm is arranged based on observing the value of negative VI in each pseudocolor range. The soil after plowing has a higher negative VI than the soil without plowing. But even so, the negative VI limit value that distinguishes cultivated and non-cultivated soil differs in each image. The process starts by classifying the VI based on pseudocolor range. The pixels with negative VI within pseudocolor range, which have higher value and more quantity, are kept as plowed areas. Otherwise, the pixels with lower pseudocolor range values and not dominant are converted to unwanted negative VI. The second segmentation algorithm is tasked with finding pixels with the higher negative VI range and having a dominant quantity. This set of pixels with negative VI is determined as the plowed area, as shown in Figure 3(c).

To determine the algorithm's accuracy, we compare the plowed area detected based on the segmentation algorithm to the plowed area based on manual observation on the ground. The comparison images are shown in Figure 4 and the comparison of the plowed area in percent is shown in Table 2. Based on this result, the correlation coefficient between the plowed area obtained from the segmentation algorithm and manual observation is 0.77.

Table 2: Percentage of The Plowed Area Based on Segmentation Algorithm and Manual Observation

Initial Image	Plowed Area (%)	
	Segmentation Algorithm	Manual Observation
Figure 1a	17%	61%
Figure 1b	35%	47%
Figure 1c	1%	3%
Figure 1d	57%	56%
Figure 1e	22%	18%
Figure 1f	7%	4%
Figure 1g	0%	0%
Figure 1h	37%	40%
Figure 1i	31%	30%

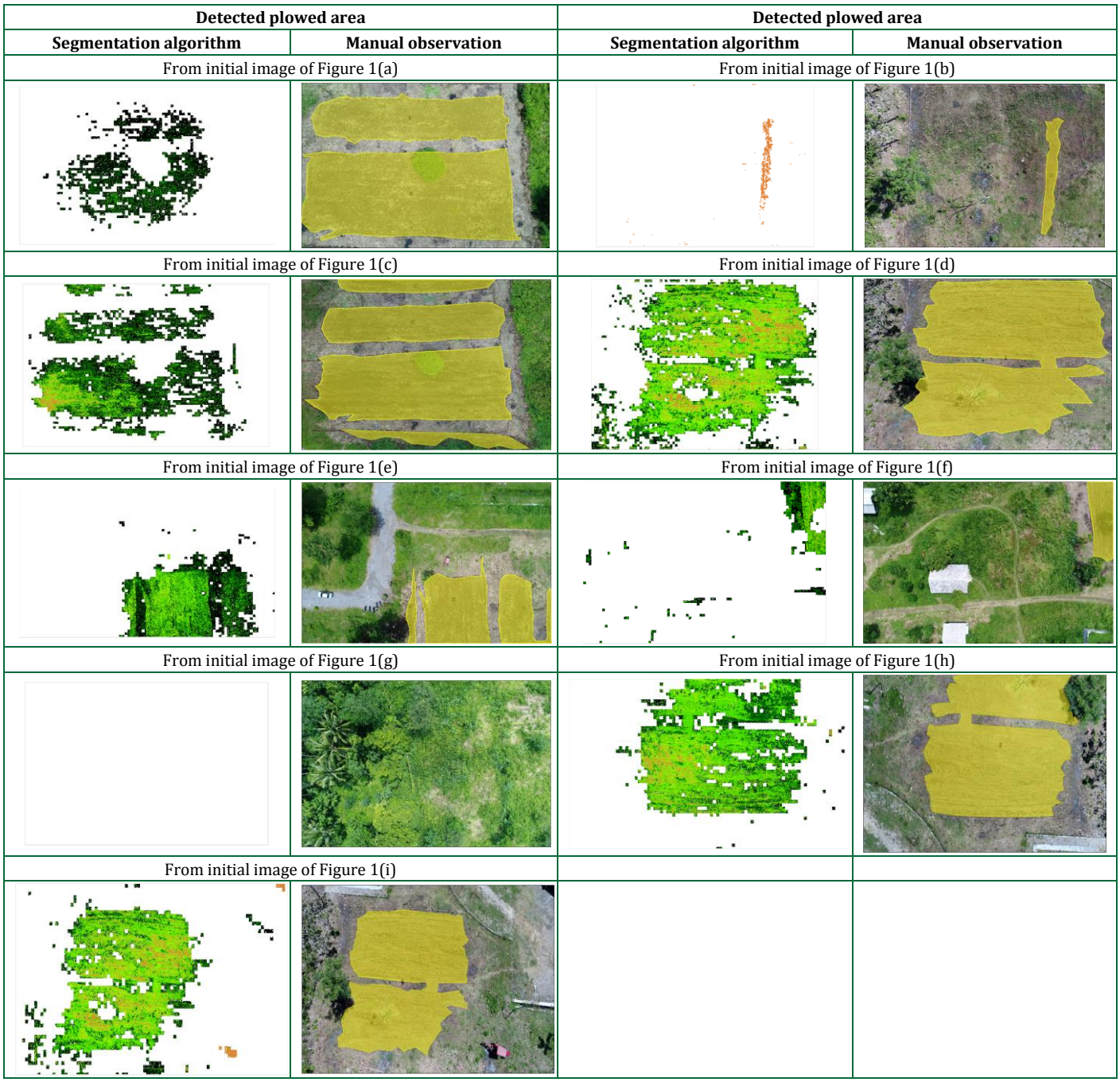

Figure 4: Image Comparison of detected plowed area based on segmentation algorithm (left) and manual observation (right)

3.3 The Plowing Depth and GLCM Measurement

Figure 5: Distribution of plowed depth measurement location

The yellow dot in Figure 5 indicates the measurement location of the plowing depth. That points measurement has been selected for representing various depth plowing. The measurement was conducted before plowing and after plowing. The GLCM parameters used in this study are contrast, energy, homogeneity, and correlation. The GLCM measurement was focused on the area with a yellow dot in the image. The correlation coefficient between GLCM parameters is shown in Table 3.

Table 3: Correlation coeffisien between plowing depth and GLCM Parameters

Correlation Coeffisien		Plowing depth	
		before plowing	after plowing
GLCM Parameters	Contrast	0.31	-0.31
	Homogeneity	-0.31	0.26
	Energy	-0.23	0.14
	Correlation	-0.19	-0.01

4. Discussion

The result of the segmentation algorithm is convincing enough based on the test that has been done. However, it must be noted that the algorithm works only based on RGB value that was converted into the vegetative index value. The most difficult is differentiating the soil before and after plowing since the negative VI value is not that different. The identifier that can be captured to distinguish between plowed and unplowed areas is mainly based on conditions of soil water content. The plowshare cuts the deeper soil layers and flips to the upper. It creates a darker color layer on the cultivated land area. The initial image of Figure 1(a) have fewer pixels with negative vegetative index (VI). It causes the plowed area has resulted

from the segmentation algorithm to be much smaller than the plowed area from manual observation.

The different results are obtained from the initial images of Figure 1(b), Figure 1(d), Figure 1(h), and Figure 1(i), which created more pixels with negative VI to be segmented. The initial image of Figure 1(b) has darker color in the plowed area, so it generates more pixels with negative VI value, which mostly range from -0.01 to -0.1. Meanwhile, the initial images of Figure 1(d), Figure 1(h), and Figure 1(i) bring out a slightly reddish color in the plowed area, which generates pixels with negative VI ranging mostly from -0.1 to -0.5. The pixels with negative VI generated from these initial images have more quantity and range than the initial image of Figure 1(b).

Since the segmentation algorithm in this study was developed based on the Vari formula to generate the vegetative index, the composition of the RGB values dramatically affects the segmentation result. The plowed soil will be easier to distinguish from unplowed soil if the pixels have higher red than green values. This is why the segmentation results of Figure 1d, Figure 1h, and Figure 1i have more initial negative VI than the result of Figure 1b. More numbers and ranges of initial negative VI values, which resulted from the Vari formula, will give better input for the segmentation process. The unplowed soil of extremely arid land usually has almost similar red, green, and blue values, which reveal the pale color of the earth. Color characteristics like this make it difficult for the algorithm to distinguish between the plowed and unplowed soil.

The investigation to find the correlation of GLCM function with the plowing depth in this study shows no correlation between the two. Although the GLCM function can characterize the image's texture, this study showed that the correlation coefficient found is extremely low. This result confirms that it is more complicated to estimate the depth on the y-axis using a 2-dimensional image. The texture characteristic of soil images tends to be similar in each coordinate, even at the points where there are significant differences in plowing depth. Based on this, GLCM cannot be further developed to estimate the plowing depth in this study.

5. Conclusion

The segmentation algorithm based on the Vari vegetative index is quite promising for detecting the plowed area. However, the GLCM function is not strong enough to estimate the plowing depth since the correlation coefficient is very weak. In addition, although the correlation coefficient of the segmentation algorithm for estimating the plowed area is quite good, this algorithm only works based on the RGB value of the image. The RGB changes are influenced mainly by changes in soil color due to differences in soil water content. The composition of red, green, and blue affects the result of the segmentation algorithm. The best results of the plowed area will be obtained on pixels with red values bigger than green so that the negative vegetative index for the segmentation process will be extensively available.

References

Al-Naji, A., Fakhri, A. B., Gharghan, S. K., and Chahl, J., 2021. Soil color analysis based on a RGB camera and an artificial neural network towards smart irrigation: A pilot study. Heliyon, 7(1), e06078. https://doi.org/10.1016/J.HELIYON.2021.E06078

ALkhafaji, A. J., Almosawi, A. A., and Alqazzaz, K. M., 2018. Performance of combined tillage equipment and it's effect on soil properties. International Journal of Environment, Agriculture and Biotechnology, 3(3), Pp.799–805. https://doi.org/10.22161/IJEAB/3.3.12

Beliakov, G., James, S., and Troiano, L., 2008. Texture recognition by using GLCM and various aggregation functions. IEEE International Conference on Fuzzy Systems, Pp. 1472–1476. https://doi.org/10.1109/FUZZY.2008.4630566

Corley, R. H. V., and Tinker, P. B., 2015. The Oil Palm: Fifth Edition. In The Oil Palm: Fifth Edition. Wiley Blackwell. https://doi.org/10.1002/9781118953297

de Amorim, F. R., Patino, M. T. O., and Santos, D. F. L., 2021. Soil tillage and sugarcane planting: an assessment of cost and economic viability. Scientia Agricola, 79(1), Pp. 1–6. https://doi.org/10.1590/1678-992X-2019-0317

Eng, L. S., Ismail, R., Hashim, W., and Baharum, A., 2019. The use of VARI, GLI, And VIgreen formulas in detecting vegetation in aerial images. International Journal of Technology, 10(7), Pp. 1385–1394. https://doi.org/10.14716/IJTECH.V10I7.3275

Fanigliulo, R., Antonucci, F., Figorilli, S., Pochi, D., Pallottino, F., Fornaciari, L., Grilli, R., and Costa, C., 2020. Light drone-based application to assess soil tillage quality parameters. Sensors (Switzerland), 20(3). https://doi.org/10.3390/S20030728

Furukawa, F., Laneng, L. A., Ando, H., Yoshimura, N., Kaneko, M., and Morimoto, J., 2021. Comparison of RGB and Multispectral Unmanned Aerial Vehicle for Monitoring Vegetation Coverage Changes on a Landslide Area. Drones 2021, Vol. 5, Page 97, 5(3), 97. https://doi.org/10.3390/DRONES5030097

Gitelson, A. A., Kaufman, Y. J., Stark, R., and Rundquist, D., 2002. Novel algorithms for remote estimation of vegetation fraction. Remote Sensing of Environment, 80(1), Pp. 76–87. https://doi.org/10.1016/S0034-4257(01)00289-9

Hartanto, R., Arkeman, Y., Hermadi, I., Sjaf, S., and Kleinke, M., 2019. Intelligent Unmanned Aerial Vehicle for Agriculture and Agroindustry. IOP Conference Series: Earth and Environmental Science, 335(1), 012001. https://doi.org/10.1088/1755-1315/335/1/012001

Louhaichi, M., Borman, M. M., and Johnson, D. E., 2008. Spatially Located Platform and Aerial Photography for Documentation of Grazing Impacts on Wheat. Http://Dx.Doi.Org/10.1080/10106040108542184, 16(1), Pp. 65–70. https://doi.org/10.1080/10106040108542184

Meng, C., Yang, W., Lan, H., Ren, X., and Li, M., 2020. Development and Application of a Vehicle-Mounted Soil Texture Detector. Sensors 2020, Vol. 20, Page 7175, 20(24), 7175. https://doi.org/10.3390/S20247175

Mira, M., Valor, E., Boluda, R., Caselles, V., and Coll, C., 2007. Influence of soil water content on the thermal infrared emissivity of bare soils: Implication for land surface temperature determination. Journal of Geophysical Research: Earth Surface, 112(F4), 4003. https://doi.org/10.1029/2007JF000749

Mohanaiah, P., Sathyanarayana, P., and GuruKumar, L., 2013. Image Texture Feature Extraction Using GLCM Approach. International Journal of Scientific and Research Publications, 3(5), Pp. 1–5. https://ijsrp.org/research-paper-0513.php?rp=P171166

Rachmat, M., Saptana, S., and Hermanto, H., 1995. Keragaan Investasi Di Subsektor Perkebunan. Forum Penelitian Agro Ekonomi, 13(1), 1–21. https://doi.org/10.21082/FAE.V13N1.1995.Pp. 1-21

Riegler, P. N., Moitzi, G., Prankl, J., Huber, J., Karner, J., Wagentristl, H., and Vincze, M., 2020. Machine vision for soil roughness measurement and control of tillage machines during seedbed preparation. Soil and Tillage Research, 196, 104351. https://doi.org/10.1016/J.STILL.2019.104351

Riegler, T., Rechberger, C., Handler, F., and Prankl, H., 2014. Image Processing System for Evaluation of Tillage Quality. LANDTECHNIK, 69(3), Pp. 125–131. https://doi.org/10.15150/LT.2014.180

Setiyono, S., Suud, H. M., Faizah, H. A., and Helwandi, I. S., 2022. The Effectivity of Image Processing Using K-Nearest Neighbor and Gray Level Co-Occurrence Matrix Method to Monitor Land Plowing Using Disc Plow. Agroteknika, 5(1), Pp. 14–25. https://doi.org/10.32530/AGROTEKNIKA.V5I1.125

Shamsabadi, H. A., 2008. Study on the effect of primary tillage practices, planting machines and different seed densities on the yield of rain-fed wheat. Asian Journal of Plant Sciences, 7(1), Pp. 79–84. https://doi.org/10.3923/AJPS.2008.79.84

Xue, J., and Su, B., 2017. Significant remote sensing vegetation indices: A review of developments and applications. Journal of Sensors, 2017. https://doi.org/10.1155/2017/1353691